Optics & Laser Technology 179 (2024) 111375

Contents lists available at ScienceDirect

Optics and Laser Technology

journal homepage: www.elsevier.com/locate/optlastec

Full length article

A mid-IR laser source for muonic hydrogen spectroscopy: The FAMU laser system

Marco Baruzzo [a,b,*], José J. Suárez-Vargas [a,b], Lyubomir I. Stoychev [a,j], Humberto Cabrera [a,c], Komlan S. Gadedjisso-Tossou [c,d,e], Guido Toci [g], Luigi Moretti [h,i], Eugenio Fasci [h,i], Livio Gianfrani [h,i], Cecilia Pizzolotto [a], Emiliano Mocchiutti [a], Miltcho B. Danailov [f], Andrea Vacchi [a,b]

[a] Sezione INFN di Trieste, via A. Valerio 2, Trieste, Italy
[b] Dipartimento di Scienze Matematiche, Informatiche e Fisiche, Università di Udine, via delle Scienze 206, Udine, Italy
[c] The Abdus Salam International Centre for Theoretical Physics, Strada Costiera 11, Trieste, Italy
[d] Laboratoire de Physique des Matériaux et des Composants à Semi-conducteurs (LPMCS), Département de Physique, Université de Lomé, 01 BP 1515 Lomé, Togo
[e] Centre d'Excellence Régional pour la Maîtrise de l'Electricité (CERME), Université de Lomé, 01 BP 1515 Lomé, Togo
[f] Elettra-Sincrotrone Trieste, SS14, km 163.5, Basovizza, Italy
[g] Consiglio Nazionale delle Ricerche, Istituto Nazionale di Ottica, CNR-INO, Via Madonna del Piano 10, Sesto Fiorentino, Italy
[h] Sezione INFN di Napoli, Complesso Universitario di Monte S. Angelo ed. 6, via Cintia, Napoli, Italy
[i] Dipartimento di Matematica e Fisica, Università della Campania "Luigi Vanvitelli", Viale Lincoln 5, Caserta, Italy
[j] Institute of Solid State Physics, Bulgarian Academy of Sciences, Tzarigradsko Chaussee Blvd. 72, 1784 Sofia, Bulgaria

ARTICLE INFO

Keywords:
Mid-IR laser
FAMU
Muonic hydrogen spectroscopy
Laser control system
DFG

ABSTRACT

A pulsed, tunable, narrow linewidth mid-infrared (mid-IR) laser radiation source was developed to meet the needs of the FAMU project (Fisica Atomi MUonici). The main goal of this experiment is to measure the hyperfine splitting of the ground state of muonic hydrogen using pulsed laser spectroscopy. The experiment requires a high energy, mid-IR source around the resonance energy $\Delta E1S_{hfs} \sim 0.1828$ eV (6.79 μm) of the muonic hydrogen atom to excite it from the para (F = 0) to the ortho (F = 1) spin state.

The laser system designed to fulfill these requirements is based on Difference Frequency Generation (DFG) using a non-linear crystal pumped by two laser beams at 1064 nm and 1262 nm. For the first time, the details of the entire laser system are described in this paper. The laser light at 6.79 μm, generated with a $BaGa_4Se_7$ non-linear crystal, is being directed into the FAMU target multi-pass optical cavity. To date, an energy above 1 mJ, a linewidth below 30 pm, and a tunability step of 9 pm have all been attained. Here, we present the unique features of the laser system and the characterization results.

1. Introduction

The FAMU (Fisica Atomi MUonici) collaboration aims to determine the proton Zemach radius by measuring the hyperfine splitting of the 1S state of the muonic hydrogen [1].

The experiment will be performed at the RIKEN-RAL facility, located in the Rutherford Appleton Laboratory (UK). The pulsed muon beam, produced by the ISIS accelerator, is brought to stop in a high purity cryogenic hydrogen gas target to form muonic hydrogen. The spin flip is induced on the thermalized 1S state by the narrow linewidth laser beam at ~0.1828 eV (6.79 μm) injected in an optical cavity inside the cryogenic gas target. The spin flip is not directly observed, but the experimental method is based on measuring the muonic transfer rate from hydrogen to a high-Z contaminant present in the target, namely, oxygen. The transfer rate is directly correlated to the energy of the muonic hydrogen. When the laser excited muonic hydrogen de-excites it gains kinetic energy and the muon transfer to oxygen increases [2,3]. When the laser is tuned at the right energy needed to excite the muonic hydrogen spin flip, a variation on the muonic transfer rate will be determined by looking at the characteristic muonic oxygen X-ray lines.

The conventional laser sources emitting in the mid-IR region, such as color center lasers, CO and CO_2 gas lasers, diode lasers and quantum cascade lasers cannot provide the laser properties required by the FAMU experiment. Light sources based on nonlinear frequency down-conversion pumped by solid-state lasers have demonstrated impressive results allowing to reach a wide range of mid-IR wavelengths combined with high energy pulses [4]. When the final setup was chosen, two

* Corresponding author at: Sezione INFN di Trieste, via A. Valerio 2, Trieste, Italy.
E-mail address: marco.baruzzo@ts.infn.it (M. Baruzzo).

https://doi.org/10.1016/j.optlastec.2024.111375
Received 12 March 2024; Received in revised form 14 June 2024; Accepted 22 June 2024
Available online 5 July 2024

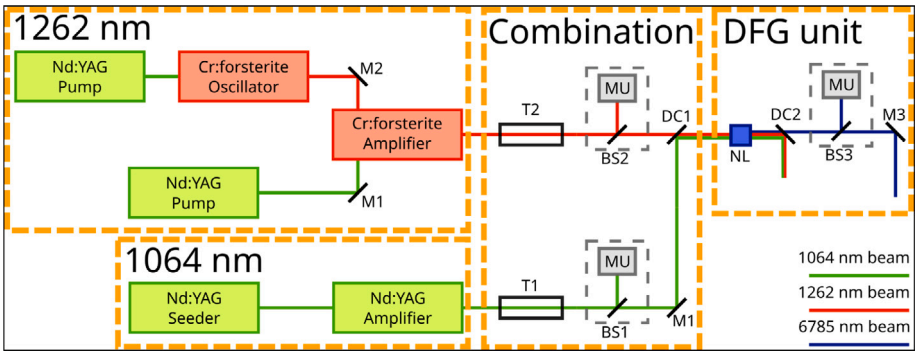

Fig. 1. Sketch of the FAMU laser system indicating the two main laser sources, the combination section and the DFG unit. (M1–M3 are Mirror, T1–T2 telescopes, BS1–BS3 beamsampler, DC1–DC2 dichroic mirror, NL nonlinear crystal and MU measuring units (wavelength meter, energy meter, dimensions)).

strategies were explored: Optical Parametric Oscillation (OPO) and Difference Frequency Generation (DFG).

OPO systems adopt a high power pump laser. They can be widely tunable and are capable to generate energies exceeding 1 mJ in the 6-10 μm range [5,6]. However, OPOs typically have large bandwidths in the order of several nm and wavelength tuning with a single mode operation requiring an active cavity adjustment. A wide tunability is rather challenging due to the need to preserve resonant cavity conditions. Moreover, in nanosecond mid-IR OPOs optimized for high energy extraction, the generation threshold is not far from the crystals' damage threshold, which poses reliability problems in cases of long duration measurements with continuous data acquisition.

The alternative scheme, based on DFG process, relies on $\chi^{(2)}$ nonlinearity too and involves three waves, namely pump, signal and idler. Compared to OPOs, the DFG process has two great advantages. First, the possibility to generate narrow bandwidth mid-IR emission by mixing narrow bandwidth pump and signal beams. Secondly, single frequency operation and continuous tuning of the DFG wavelength can be easily obtained at a fixed pump wavelength by tuning the signal wavelength and by rotating the non-linear (NL) crystal to the corresponding phase-matching angle.

Recent developments in ultrafast femtosecond laser sources have significantly emphasized DFG and OPA-based new mid-IR laser media. Recent studies highlight promising applications in OPA using Ce-doped chalcogenides [7], Cr:ZnSe [8], and in DFG applications with Fe:ZnSe and Fe:CdSe [9] and ZGP crystals [10]. These advancements enable high-energy mid-IR pulse generation, potentially reaching our target wavelength range of around 6-7 μm. Utilizing ns-pulsed lasers to pump similar setups can reduce the linewidth to the level required for the FAMU experiment, potentially offering alternative solutions to enhance the current laser scheme.

This work describes the DFG-based laser system, expressly developed for the FAMU experiment, which emits a 7 ns pulsed radiation with a repetition rate of 25 Hz, an energy peak of 1.3 mJ, a linewidth of less than 30 pm and tunable between 6730 and 7135 nm. These characteristics make the laser a unique source of coherent radiation in our region of interest.

2. FAMU laser setup

The solution chosen to produce the radiation required by the FAMU experiment is the DFG process, which can provide a tunable, narrow linewidth, high energy mid-IR light pulses. The DFG requires two different single mode laser sources that have to be combined before being injected in the non linear crystal. The two wavelengths selected for this application are 1064 nm as pump beam and 1262 nm as signal beam, which are then combined and monitored before being injected in the DFG unit for the generation and monitoring of the 6.79 μm light. Fig. 1 schematically illustrates the system.

The generated 6.79 μm light is then coupled to the FAMU gas target, which is equipped with a multi-pass optical cavity. The entire laser system is installed on an optical table covered by a nonflammable plastic interlocked box aimed to satisfy both safety and thermal stabilization needs, thus increasing the stability of the entire laser system. The temperature inside the interlocked box is stable with fluctuations of 0.5 °C. All crystals, except the NL crystal, are actively cooled with a water heat sink and chilled water.

2.1. The 1064 nm laser beam

The pump of the DFG system is provided by a commercially available injection-seeded single-longitudinal mode (SLM) Nd:YAG laser system centered at 1064.426 nm, properly modified to meet the experiment specific requirements about the pulse duration. This is a master-oscillator power-amplifier (MOPA) Nd:YAG laser system (INNOLAS SpitLight Hybrid II), seeded with a highly stable continuous-wave fiber laser at 1064.4305 nm (Rock Fiber Laser Seeder, NP Photonics), with feedback controlled piezomotor system which enables to keep the single longitudinal mode, with a 0.35 pm line-width.

The wavelength stability is improved by the feedback controlled piezomotor system. The standard deviation of the wavelength distribution in an hour of measurements is typically of 0.3 pm. The drift of the mean value of the wavelength distribution during a week, shown in Fig. 2, is close to 1 pm. This laser source is able to provide up to 140 mJ pulses, with a pulse duration of 18–22 ns and time jitter of less than 1 ns, triggered at 25 Hz rate.

2.2. The 1262 nm laser beam

The laser beam used as signal in the DFG process is centered at 1262 nm and can be tuned in a range between 1257–1267 nm with a line-width smaller than 0.8 pm. Emitting on a single longitudinal mode, this laser provides pulses with duration of 9 ns, energy up to 45 mJ and a time jitter of ±2.5 ns.

This 1262 nm laser beam is produced by a dedicated Cr:forsterite MOPA laser system containing a Cr:forsterite crystal, pumped by a built-in Nd:YAG laser (LS-2138N, LOTIS TII). The generated light is then injected in a 3-stage, 16-pass power-amplifier, pumped by another Nd:YAG laser (INNOLAS SpitLight 600, ~ 530 mJ).

The Cr:forsterite oscillator, shown in Fig. 3, consists of a dichroic input mirror (1), a 6.5 × 9 × 16 mm Cr:forsterite crystal (2), a beam expanding right-angle prism to protect the diffraction grating (3), a diffraction grating (4) and a back mirror (5). The dispersed beam coming out from the prism is deviated with high precision in the 1st diffraction order of the grating, thus forming a grazing incidence cavity, with the 0th order providing the output beam of the oscillator, sent to the amplifier. The back mirror (5) is placed on a piezo-controlled rotation stage, thus allowing the selection of the required wavelength

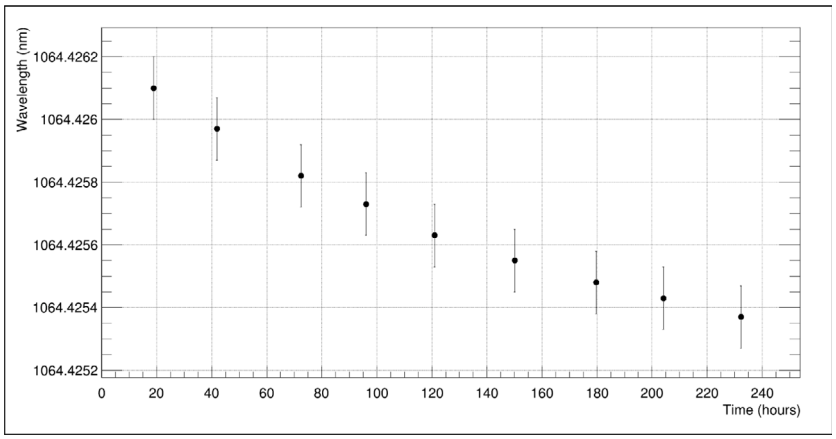

Fig. 2. The plot shows the wavelength vs time data for the INNOLAS SpitLight Hybrid II from the startup of the laser. The plot covers more than a week of data taking. The errors are the standard deviations of the wavelength distribution.

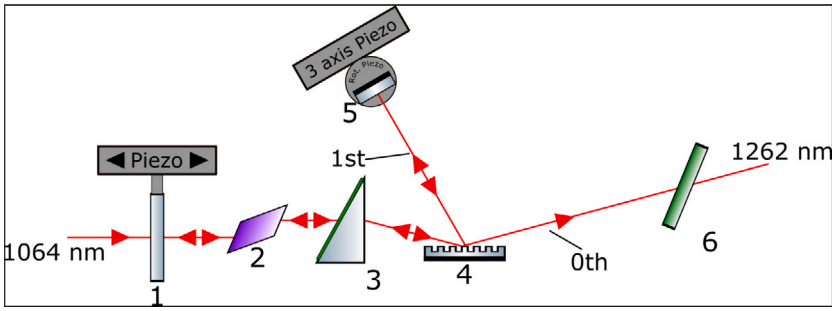

Fig. 3. Cr:forsterite oscillator scheme: dichroic input mirror (AR@1064 nm, HR R> 99@1262 nm)(1), Cr:forsterite crystal (2), right-angle beam-expanding prism (3), diffraction grating (1350 grooves/mm)(4) and back mirror (HR R> 99@1257–1267 nm)(5), and output window placed at 56° with respect to the beam (6).

by changing its angle with respect to the 1st diffraction order. The whole assembly is fixed on a kinematic mirror mount with piezoelectric adjusters that allows one to control the cavity alignment of the Cr:forsterite cavity. The total Cr:forsterite oscillator cavity length is about 168 mm. Further details on the oscillator cavity can be found in [11,12].

Thermal and mechanical effects generate the instability of the Cr:forsterite oscillator's cavity and the loss of the single mode operation of the laser emission.

To mitigate this problem the oscillator is paired to an on purpose developed software (FAMU Laser Control or FLC), which monitors and controls the parameters of the entire laser in real time through a series of sensors and piezomotors. In the case of the oscillator, the program has specific functions to maintain the single mode operation (Single Mode Keeper or SMK) and the constant wavelength (WaveLength Keeper or WLK). These functions act automatically on the piezomotors of the dichroic input mirror and on the vertical adjuster of the back mirror (both shown in figure Fig. 3) using the measurements collected in real time by the program as input. The SMK uses the time required by the laser beam to form in the oscillator cavity collected with a PIN-photodiode (EOT InGaAs ET-3010, connected to an oscilloscope) as the trigger parameter for the single mode operation maintainer.

A notable feature of the program is the WLK that keeps the wavelength constant by adapting the oscillator cavity length in a continuous closed loop. Laser stability increases significantly in terms of wavelength, single mode and linewidth, while at the same time decreasing the number of direct user actions of the laser. WLK uses the wavelength and the linewidth measured with a wavelength meter (High Finesse, model WS7-600 IR-I) as parameters .

FLC also monitors energy (Coherent Inc., model EnergyMax-USB J-50MB-LE), beam size and position (CMOS camera acA2440-20gc, Basler AG) of the oscillator before entering in the amplifier. An example of the FLC graphic interface, in Fig. 4, shows from left the image of the laser beam, some trends of the various oscillator parameters, e.g energy and wavelength, and the laser pulse temporal shape. All these measurements are collected 5 times per second.

With a pump energy of 50 mJ, the oscillator generates approximately 1 mJ in the spectral range 1257–1267 nm, thus preserving the energy output of the Cr:forsterite amplifier and of the DFG setup as a whole. The 1262 nm light produced by the oscillator is injected in the amplifier unit pumped by another Nd:YAG laser (INNOLAS SpitLight 600), in order to increase the final energy by a factor of 50 and more. Fig. 5 shows the optical layout of the multipass amplifier.

Three stages constitute the structure of the uniquely developed optical amplifier, each one equipped with a Cr:forsterite crystal, cut at Brewster angle, for a total of 16 passes through all of them. The 3 crystals have different dimensions and are pumped with different energies from a Nd:YAG laser at 1064 nm. The latter delivers a total of 450 mJ of horizontally polarized light, which is split in three parts using a set of waveplates and polarizers. The energies injected in the crystals are 112 mJ in the first crystal, 156 mJ in the second and 160 mJ in the third. These energy values are chosen to keep the energies of the three pump beams close to the optimal excitation energy density of 1 J/cm^2. The first two crystals undergo six passes of the 1262 nm laser each, while the last crystal sees only four passes, due to the depletion of the stored pump energy that is caused by the 1262 nm laser coming from the second stage [12].

A total output energy close to 45 mJ is generated starting from a 0.85 mJ oscillator beam thus giving a multiplication factor of 53. Using the same pump energies reported, the energies produced by each stage are 5.2 mJ in the first stage, 25.5 mJ in the second and 43.5 mJ in the third. A complete description and characterization of this amplifier can be found in [11,12].

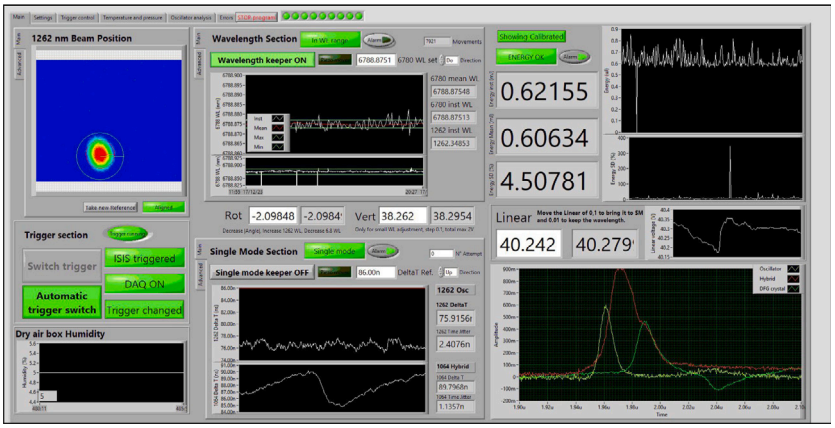

Fig. 4. 1262 nm oscillator control interface. From top left clockwise, the window shows the shape and position of the laser beam collected with a camera, the measurement of the wavelength and the laser energy with graphs of their stability. In the lower part there are the laser pulses collected by the photodiodes with on the right the trend of the time to form the laser beam. In the central part of the window there are controllers for modifying the positions of the piezomotors and for activating the automatic functions.

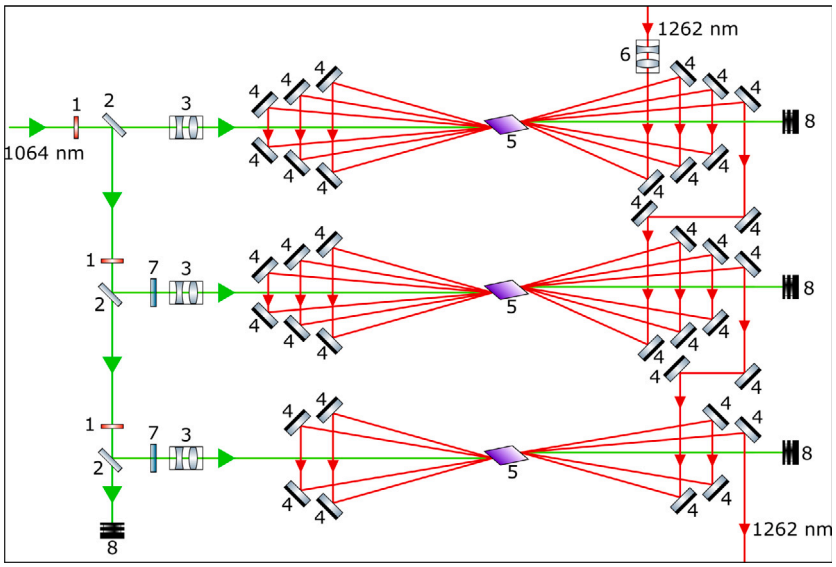

Fig. 5. 1262 nm amplifier unit: $\lambda/2$ waveplate at 1064 nm(1), polarizer at 1064 nm(2), telescope AR coated at 1064 nm(3), mirror HR 1262 nm(4), Cr:forsterite crystal (5), telescope AR 1262 nm(6), polarization rotator 90° at 1064 nm(7) and beam dump (8).

Because of the progressive temperature stabilization of the whole system, the wavelength of the amplified 1262 nm beam reaches a stable value after about 8 h from the laser power on. The laser tunability step is of the order of 0.1 pm and it is obtained with a specifically developed procedure moving all the Cr:forsterite oscillator piezomotors.

2.3. Combining the two beams

The DFG process requires time synchronization and superposition of the 1064 nm and 1262 nm beams at the NL crystal.

A pulse generator (Quantum Composer, model 9520) triggers both lasers flashlamps and Pockels cells, allowing the time synchronization of the beams. A PIN-photodiode collects the two laser pulses together and provides the potential delay between the pulses. The intrinsic instability of the Cr:forsterite oscillator forced us to increase the 1064 nm pulse width to 18 ns to ensure the optimal synchronization inside the DFG crystal.

Dedicated telescopes (showed in Fig. 1 as T1 and T2) resize the 1064 nm and 1262 nm beams to 6.2 and 5.5 mm respectively, in order to fit the NL crystal. Beams sections are TEM00 mode as shown in Fig. 6. The beams are superimposed with a dichroic mirror. A system of mirrors, of which two are mounted on piezo driven tip/tilts (PI-Physik Instrumente, model S-330.2SH, High-Dynamics Piezo Tip/Tilt Platform), enables a precise and remote alignment of the beams. A pair of beam samplers direct a portion of each beam to two NIR cameras, thus allowing an online control of the beams relative positions and transverse dimensions. With each camera, an energy meter and a wavelength meter perform online measurements of energy, wavelength and linewidth to monitor the status of both lasers before entering the NL crystal.

2.4. DFG scheme

To achieve the FAMU requirements the Nd:YAG is set at 1064.426 nm and the Cr:forsterite is tuned around 1262.290 nm, thus generating the mid-IR radiation at the wavelength of 6789 nm [13]. The NL crystal is fixed on a 6 axis kinematic mount to align it and to set the correct phase-matching angle. Fig. 7A shows a single pass configuration which is used during the first FAMU data acquisition. Fig. 7B represents a scheme of a double pass configuration that will be implemented to increase the energy [14].

A series of nonlinear crystals of different materials were tested using the FAMU laser DFG unit to determine the optimum choice

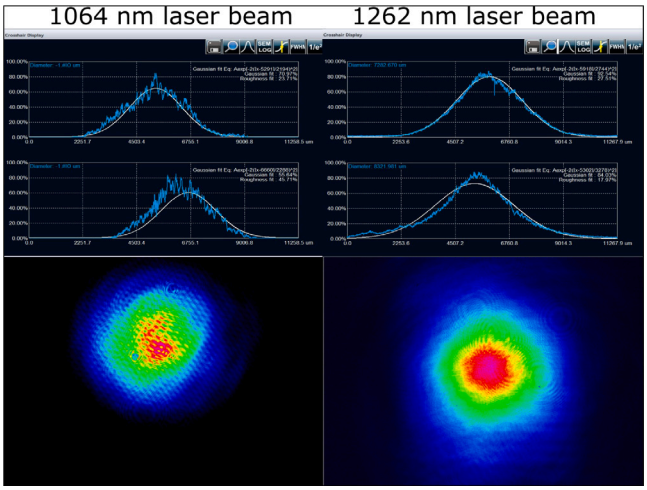

Fig. 6. Images of the transverse mode of both beams with the energy distribution along X and Y axis. The beam profile of the 1064 nm radiation presents interfering patterns as we have used a set of neutral filters to decrease its intensity.

that achieve the maximum possible energy. The final choice, dictated also by reasons of practical use and crystal availability, turned out to be a 8.9 × 10.3 × 28.5 mm^3 $BaGa_4Se_7$ crystal type-I, ee-o phase matching, with a damage threshold of 557 MW/cm^2. During the final characterization of the crystal, some non-critical internal defects were evident in this crystal. This did not prevent its use, but forced us to take special care about the injected energy to prevent damage. The 6.79 μm laser beam is monitored to control the wavelength, linewidth and energy of the laser beam on every shot which is injected into the cryogenic target. This data is saved on the PC and then collected by the FAMUAnalysis program, which performs a real time first check of the data collected from all detectors of the experiment.

One of the key points of the FAMU experiment is the accuracy of the laser wavelength measurement. To this purpose, a frequency calibration procedure was developed exploiting the absorption features of gaseous ethylene (C_2H_4) in the mid-IR. A gas cell is filled and placed on the path of the 6.79 μm beam. Light absorption is then measured comparing the energies before and after the cell. The absorption spectrum that is obtained by tuning the laser wavelength is compared to the HITRAN [15] database, thus leading to a the calibration of the laser frequency in the mid-IR.

To avoid absorption of the IR light in air, caused by atmospheric water vapor, the DFG setup and the light path to the target are enclosed in tight covers filled with dry air, keeping the internal atmosphere at below 5% RH. At this point the generated mid-IR beam at 6.79 μm, after being characterized, is sent to the FAMU target.

3. Mid-IR laser characterizations

The 6.79 μm laser beam produced with the $BaGa_4Se_7$ was selected with a tri-chroic mirror and injected in an energy meter (Coherent Inc., model EnergyMax-USB J-10MB-LE) which measured a maximum average energy of 1.2 ± 0.06 mJ when injecting 24 mJ at 1064 nm and 24 mJ at 1262 nm. The peak energy was 1.3 mJ and the stability over a time span of about one hour was 5%. This energy is evaluated as sufficient for the initial operation of the FAMU experiment. Other important features are the covered spectral range and the linewidth. These quantities were measured by using a wavelength meter (High Finesse, model WS6 IR-III). Fig. 8 shows that we could cover the wavelength range between 6730 and 7135 nm, with a linewidth of less than 30 pm on the entire spectral range, this latter measurement being limited by the instrument resolution. The required spectral range for the experiment is 6789 ± 3 nm, much shorter than the full instrument range and it can be compared with the measured nonlinear bandwidth FWHM of 35 nm at 6795 nm with and angular bandwidth of less than a 0.2°. The minimum tunability step at 6.79 μm is of the order of 1 pm.

Table 1
FAMU laser requirements and experimental results.

Parameters	FAMU requirements	Present results
Wavelength	6789 ± 3 nm	6730–7135 nm
Energy output	>1 mJ	1.2 mJ
Line-width	<0.07 nm	< 0.03 nm
Tunability step	0.03 nm	0.009 nm
Pulses duration	10 ns	7 ns
Repetition rate	25 Hz	25 Hz
Laser spectrum	SLM	SLM

An example of the stability of the laser wavelength is shown in Fig. 9 and Fig. 10, which respectively represent the trend of the wavelength during a measurement of 24 h and the distribution of the wavelength measured in the same time period. The trend plot shows a stable wavelength throughout almost the entire measurement, except for a single event where the laser lost the required wavelength, but the team managed to re-tune it. The wavelength distribution clearly peaks at 6785.875 nm, with a standard deviation of 3 pm.

To further test the laser tunability and wavelength measurement capability, an absorption spectrum of the water humidity in the laboratory air was collected. The moisture level during the acquisition of this data was between 40 and 45% RH (Relative Humidity). The focus was set on the absorption peaks in the wavelength range close to the experimental configuration, i.e. between 6769 and 6798 nm. The wavelength values were calculated from the measured wavelengths of the 1262 nm beam and keeping the wavelength of the 1064 nm beam constant at 1064.4305 nm. The wavelength was tuned changing the angle of the piezocontrolled rotation stage in the Cr:forsterite oscillator. The humidity absorption was measured as the ratio of laser pulse energy at two different distances and normalized to obtain the fractional absorption. No changes or calibrations were performed on the wavelength axis. The results of the measurement are shown in Fig. 11 in comparison with the calculated HITRAN [15] absorption spectrum of air with 30% RH moisture. The peaks can be recognized in the correct positions at first glance with comparable amplitude. This test confirmed the optimal measurement of the wavelength and the tunability capability of the laser in the experiment wavelength range.

4. Conclusion

A mid-IR, tunable, narrow bandwidth laser source emitting around 6.79 μm was developed for the FAMU experiment. The aim of the experiment is to measure the proton radius by measuring the hyperfine splitting of 1S state for muonic hydrogen atom. The laser is required to excite the transition in the muonic hydrogen. It is based on a DFG scheme pumped by a fixed light source at 1064 nm and a tunable laser around 1262 nm, allowing the generation of infrared radiation in the spectral range 6730–7135 nm.

The FAMU laser system fulfills the experiment's requirements, as shown in Table 1, and, to the best of our knowledge, it represents a unique source at this wavelength with a linewidth smaller than 30 pm and an energy up to 1.3 mJ. The laser light will be coupled to the optical cavity, which is fixed inside the cryogenic target of FAMU, allowing to perform the experiment. The future plans foresee an upgrade of the Cr:forsterite oscillator laser with the aim to optimize the stability and reliability with an Optical Parameter Oscillator (OPO) pumped by the same Nd:YAG laser pump used by the DFG setup [16]. Such an upgrade is expected to further increase the 6.79 μm pulse parameters stability and tunability. It is envisioned that the upgraded system may address wider area of applications, including minimally invasive brain surgery [17] and biochemical analysis [18].

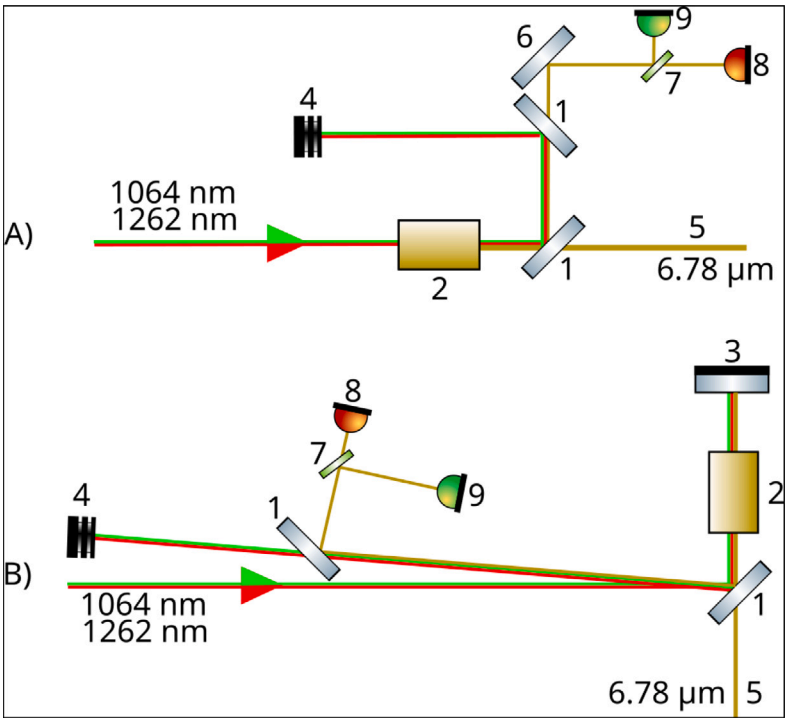

Fig. 7. Panel A is a diagram of the DFG setup in single pass and while panel B reports a double pass configurations with absolute calibration. The two sketches include: tri-chroic mirror (1), NL crystal (2), silver mirror (3), beam dump (4), mid-IR laser beam (5), mid-ir mirror (6), beam splitter (7), energy meter (8), mid-ir photodiode (9).

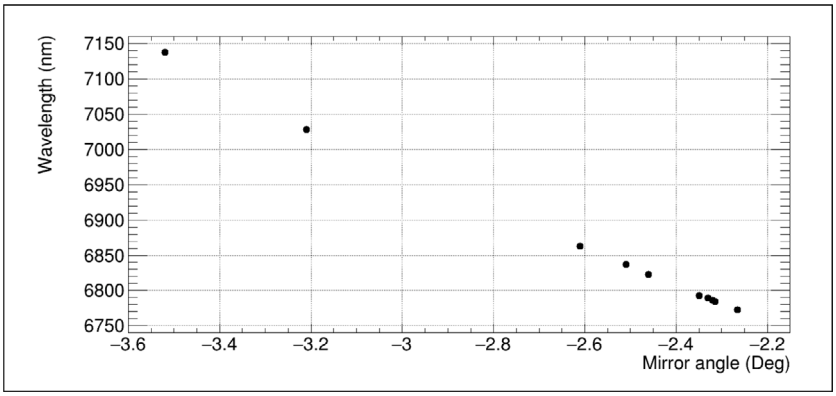

Fig. 8. The laser wavelength interval between 6750–7135 nm reachable by moving the piezo-controlled rotation stage. The error bars are inside the points.

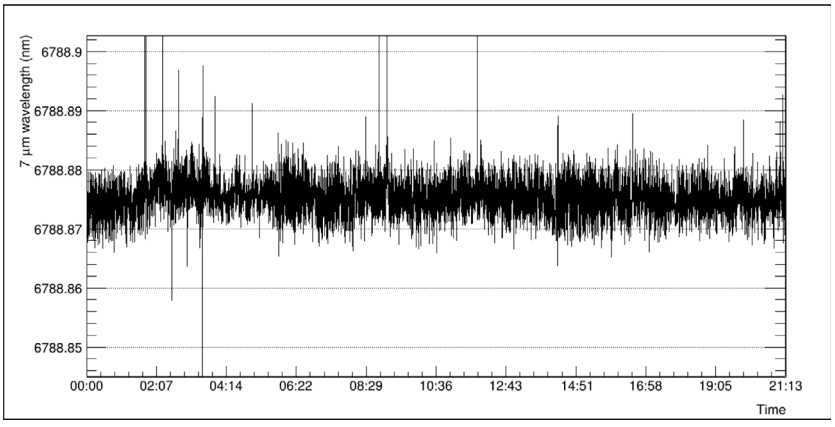

Fig. 9. A wavelength-vs-time plot of the wavelength stability test. The spikes due to temporary loss of single mode.

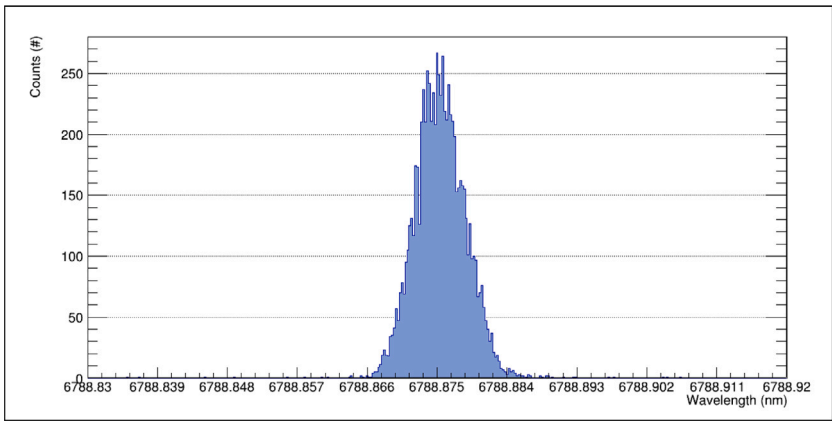

Fig. 10. The distribution of the laser wavelength at 6.79 μm during a stability test. The standard deviation is 3 pm.

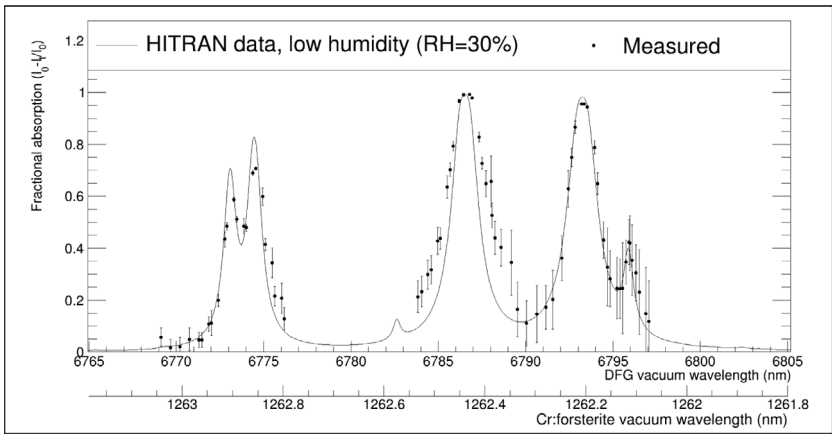

Fig. 11. The air humidity absorption spectrum in the 6769–6798 nm collected with the FAMU laser system in 100 cm. The air humidity was between 40 and 45% RH. The absorption coefficients are calculated from the ratio of the beam energies at two different distances and normalized conveniently. The 6.79 μm wavelength values are calculated from the measured 1064 nm and 1262 nm wavelength beams.

CRediT authorship contribution statement

Marco Baruzzo: Writing – review & editing, Writing – original draft, Visualization, Validation, Supervision, Software, Resources, Methodology, Investigation, Formal analysis, Data curation, Conceptualization. **José J. Suárez-Vargas:** Writing – review & editing, Writing – original draft, Validation, Supervision, Resources, Methodology, Investigation, Data curation, Conceptualization. **Lyubomir I. Stoychev:** Writing – review & editing, Supervision, Methodology, Investigation, Conceptualization. **Humberto Cabrera:** Writing – review & editing, Methodology, Investigation, Conceptualization. **Komlan S. Gadedjisso-Tossou:** Writing – review & editing, Investigation. **Guido Toci:** Writing – review & editing, Methodology, Conceptualization. **Luigi Moretti:** Writing – review & editing, Validation, Methodology, Investigation, Data curation, Conceptualization. **Eugenio Fasci:** Writing – review & editing, Validation, Methodology, Investigation, Data curation, Conceptualization. **Livio Gianfrani:** Writing – review & editing. **Cecilia Pizzolotto:** Writing – review & editing, Resources, Project administration, Funding acquisition. **Emiliano Mocchiutti:** Writing – review & editing, Resources, Project administration, Funding acquisition. **Miltcho B. Danailov:** Writing – review & editing, Supervision, Resources, Methodology, Conceptualization. **Andrea Vacchi:** Writing – review & editing, Supervision, Resources, Project administration, Funding acquisition, Conceptualization.

Data availability

The authors are unable or have chosen not to specify which data has been used.

Acknowledgment

The authors would like to express gratitude to INFN and Elettra for support of this work, and in particular, the SPIE- ICTP Anchor Research Program funded generously by the International Society for Optics and Photonics (SPIE).

References

[1] D. Bakalov, E. Milotti, C. Rizzo, A. Vacchi, E. Zavattini, Experimental method to measure the hyperfine splitting of muomic hydrogen (μ-p)1S, Phys. Lett. A 172 (1993) 277–280, http://dx.doi.org/10.1016/0375-9601(93)91021-V.

[2] C. Pizzolotto, A. Adamczak, et al., The FAMU experiment: muonic hydrogen high precision spectroscopy studies, Eur. Phys. J. A 56 (2020) 185, http://dx.doi.org/10.1140/s10050-020-00195-9.

[3] M. Stoilov, A. Adamczak, et al., Experimental determination of the energy dependence of the rate of the muon transfer reaction from muonic hydrogen to oxygen for collision energies up to 0.1 eV, Phys. Rev. A 107 (2023) 3, http://dx.doi.org/10.1103/PhysRevA.107.032823.

[4] V. Petrov, Frequency down-conversion of solid-state laser sources to the mid-infrared spectral range using non-oxide nonlinear crystals, Prog. Quantum Electron. 42 (2015) 1–106, http://dx.doi.org/10.1016/j.pquantelec.2015.04.001.

[5] M. Gerhards, High energy and narrow bandwidth mid IR nanosecond laser system, Opt. Commun. 241 (2004) 493–497, http://dx.doi.org/10.1016/j.optcom.2004.07.035.

[6] G. Stoeppler, N. Thilmann, V. Pasiskevicius, A. Zukauskas, C. Canalias, M. Eichhorn, Tunable mid-infrared $ZnGeP_2$ RISTRA OPO pumped by periodically-poled Rb:KTP optical parametric master-oscillator power amplifier, Opt. Express 20 (4) (2012) 4509–4517, http://dx.doi.org/10.1364/OE.20.004509.

[7] M.P. Frolov, S.O. Leonov, Y.V. Korostelin, V.I. Kozlovsky, Y.K. Skasyrsky, M.V. Sukhanov, A.P. Velmuzhov, P. Fjodorow, B.I. Galagan, B.I. Denker, S.E. Sverchkov, V.V. Koltashev, V.G. Plotnichenko, Current progress in Ce-doped selenide glasses for mid-infrared lasers, Opt. Mater. Express 12 (12) (2022) 4619–4629, http://dx.doi.org/10.1364/OME.472550.

[8] S.-H. Nam, V. Fedorov, S. Mirov, K.-H. Hong, Octave-spanning mid-infrared femtosecond OPA in a ZnGeP2 pumped by a 2.4 μm Cr:ZnSe chirped-pulse amplifier, Opt. Express 28 (22) (2020) 32403–32414, http://dx.doi.org/10.1364/OE.405648.

[9] A. Pushkin, E. Migal, D. Suleimanova, E. Mareev, F. Potemkin, High-power solid-state near- and Mid-IR ultrafast laser sources for strong-field science, Photonics 9 (2) (2022) http://dx.doi.org/10.3390/photonics9020090.

[10] X. Su, R. Zhu, B. Wang, Y. Bai, T. Ding, T. Sun, X. Lü, J. Peng, Y. Zheng, Generation of 8–20 μm mid-infrared ultrashort femtosecond laser pulses via difference frequency generation, Photonics 9 (6) (2022) http://dx.doi.org/10.3390/photonics9060372.

[11] L.I. Stoychev, H. Cabrera, K.S. Gadedjisso-Tossou, I.P. Nikolov, P. Sigalotti, A.A. Demidovich, J.J. Suárez-Vargas, E. Mocchiutti, J. Niemela, M. Baruzzo, N. Vasiliev, Y. Zaporozhchenko, M.B. Danailov, A. Vacchi, Pulse amplification in a Cr4+:forsterite single longitudinal mode (SLM) multi-pass amplifier, Laser Phys. 29 (6) (2019) 065801, http://dx.doi.org/10.1088/1555-6611/ab17cf.

[12] L.I. Stoychev, H. Cabrera, K.S. Gadedjisso-Tossou, N. Vasiliev, Y. Zaporozhchenko, I.P. Nikolov, P. Sigalotti, A.A. Demidovich, J.J. Suárez-Vargas, E. Mocchiutti, C. Pizzolotto, J. Niemela, M. Baruzzo, M.B. Danailov, A. Vacchi, 24 mJ Cr+4:forsterite four-stage master-oscillator power-amplifier laser system for high resolution mid-infrared spectroscopy, Rev. Sci. Instrum. 90 (9) (2019) 093002, http://dx.doi.org/10.1063/1.5115105.

[13] L.I. Stoychev, M.B. Danailov, A.A. Demidovich, I.P. Nikolov, P. Cinquegrana, P. Sigalotti, D. Bakalov, A. Vacchi, DFG-based mid-IR laser system for muonic-hydrogen spectroscopy, in: Laser Sources and Applications II, vol. 9135, International Society for Optics and Photonics, SPIE, 2014, pp. 52–57, http://dx.doi.org/10.1117/12.2052110.

[14] L.I. Stoychev, H. Cabrera, J.J. Suárez-Vargas, M. Baruzzo, K.S. Gadedjisso-Tossou, I.P. Nikolov, P. Sigalotti, A.A. Demidovich, E. Mocchiutti, C. Pizzolotto, J. Niemela, G. Toci, M.B. Danailov, A. Vacchi, DFG-based mid-IR tunable source with 0.5 mJ energy and a 30 pm linewidth, Opt. Lett. 45 (19) (2020) 5526–5529, http://dx.doi.org/10.1364/OL.405272.

[15] HITRAN, https://hitran.org/.

[16] L. Velarde, D.P. Engelhart, D. Matsiev, J. LaRue, D.J. Auerbach, A.M. Wodtke, Generation of tunable narrow bandwidth nanosecond pulses in the deep ultraviolet for efficient optical pumping and high resolution spectroscopy, Rev. Sci. Instrum. 81 (6) (2010) 063106, http://dx.doi.org/10.1063/1.3436973.

[17] J.T. Walsh Jr., T.J. Flotte, R.R. Anderson, T.F. Deutsch, Pulsed CO_2 laser tissue ablation: Effect of tissue type and pulse duration on thermal damage, Lasers Surg. Med. 8 (2) (1988) 108–118, http://dx.doi.org/10.1002/lsm.1900080204.

[18] T.I. T. Kawasaki, K. Tsukiyama, Se of a Mid-Infrared Free-Electron Laser (MIR-FEL) for dissociation of the amyloid fibril aggregates of a peptide, J. Anal. Sci. Methods Instrum. 4 (2014) 9–18, http://dx.doi.org/10.4236/jasmi.2014.41002.